



Studies of multi-pixel Geiger-mode MRS APDs for muon veto scintillator detectors of cryogenic experiments

R. FALKENSTEIN¹, V.M. GOLOVIN³, P. GRABMAYR¹, J. JOCHUM¹, B.K. LUBSANDORZHIEV^{1,2}, N.B. LUBSANDORZHIEV², R.V. POLESHUK², F. RITTER¹, CH. SAILER¹, B.A. SHAIBONOV (JR)², K. VON STURM¹.

¹*Kepler Centre for Astro and Particle Physics, University of Tuebingen, Tuebingen, Germany*

²*Institute for Nuclear Research of the Russian academy of Sciences, Moscow, Russia*

³*Centre of Perspective Technology and Apparatus (CPTA), Moscow Russia*

lubsand@rambler.ru DOI: 10.7529/ICRC2011/V04/1054

Abstract: In this paper, we present results of extensive studies of multi-pixel Geiger-mode avalanche photodiodes (MRS APDs) used in plastic scintillator muon veto detectors of cryogenic experiments.

Keywords: Multi-pixel Geiger-mode avalanche photodiodes, MRS APD, plastic scintillators, WLS fibres.

1 Introduction

Two astroparticle physics low background experiments are located in the underground laboratory of the University of Tübingen. In order to shield them against cosmic ray muons, active muon veto detectors will be installed. Both of the muon veto systems will be constructed using plastic scintillator panels. Each panel contains a wavelength shifting fibre (WLS) which is embedded in a U-shaped groove. Both ends of the fibre are read out by multi-pixel Geiger-mode avalanche photodiodes (MRS APDs). Extensive studies of the main parameters of MRS APDs, e.g. breakdown voltages, gain and parameters temperature dependencies have been carried out.

2 Multi-pixel Geiger-mode avalanche photodiodes (MRS APDs)

Multi-pixel avalanche photodiodes working in a restricted Geiger mode have been getting intense development for the last two decades [1-5]. They consist of many micro-cells on the common silicon substrate, which are connected in parallel. Each micro-cell is connected in series with a quenching resistor. The device has a metal-resistor semiconductor layer structure and is operated in the limited Geiger-mode. The multi-pixel Geiger-mode APD used for our experiments are produced by CPTA, Moscow. For further details on MRS APDs the reader is referred to [6,7].

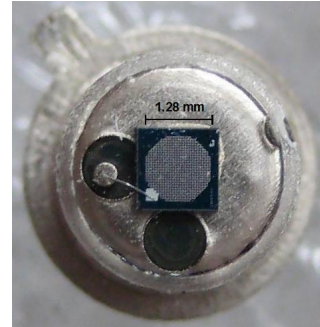


Figure 1: Photograph of a MRS APD.

The sensitive area of the MRS APD has an octagonal shape with 1.28 mm between opposed sides and is protected by an epoxy layer (see figure 1). The device consists of 796 pixels and it is packaged in a common metal TO-18 enclosure. The sensitive micro-cells of $40 \times 40 \mu m^2$ size are divided by grooves, filled with an optical nontransparent material in order to suppress optical crosstalk between the pixels [7]. The MRS APD is based on a n^+pp^+ doping layer structure as can be seen in figure 2. This structure leads to a high electric field gradient in the zone around the thin ($\sim 1 \mu m$) n^+p junction. This is the region where the avalanche multiplication of the photoelectrons occurs, however the generation of the photoelectrons mainly occurs in the p but also in the n^+ regions. The structure of the MRS APD used in this work is optimized for the detection of light in the green and red part of the optical spectrum.

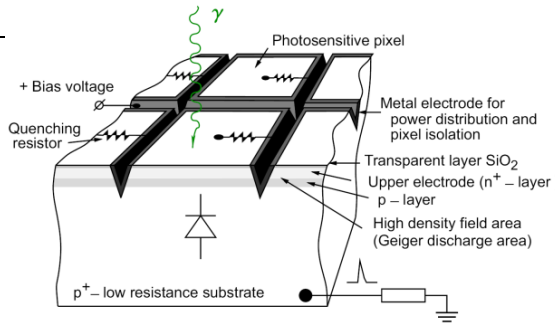


Figure 2: Simplified topology of the MRS APD [6,7].

MRS APDs have a high internal gain, which is almost comparable to that of vacuum photomultipliers. Each micro-cell of a MRS APD can be represented by a microcapacitor C_{pixel} . If now a breakdown occurs in one of the cells, it promptly discharges until such time as the voltage across it has decreased below the breakdown voltage. From this it follows that the total amount of charge flowing out of the microcapacitor during the breakdown is given by:

$$Q_{pixel} = C_{pixel} \cdot (V_{bias} - V_{bd})$$

where C_{pixel} is the capacitance of a single pixel and V_{bd} the breakdown voltage. The internal gain is thus given by:

$$G = Q_{pixel}/e$$

where e is the electron charge.

The photon detection efficiency (PDE) of a MRS APD is the ratio of the detected number of photons to the number of incident photons. It is the product of three parameters:

$$PDE = QE \cdot \epsilon_{geom} \cdot \epsilon_{Geiger}$$

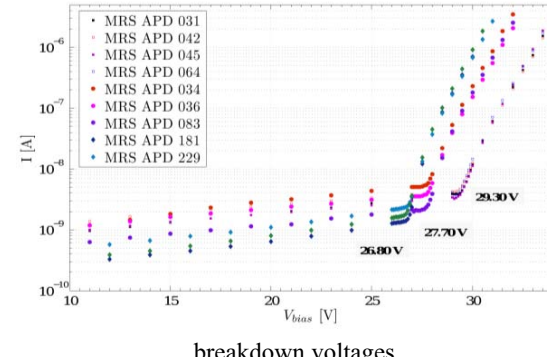
where QE is the quantum efficiency, ϵ_{geom} the geometric factor and ϵ_{Geiger} the overvoltage-dependent probability that a photoelectron or hole triggers a Geiger discharge in silicon. The geometric factor is entirely defined by the topology of the MRS APD. It is given by the ratio of the sensitive area of all pixels combined, to the total surface of the element and has a value of $\epsilon_{geom} \sim 0.6-0.7$ [6,7]. The PDE of the MRS APDs is about 25-30% at 515 nm in average [7].

3 I-V measurements

All of the MRS APDs (~ 300) were first characterized by measuring their reverse current-voltage characteristics (I-V curves) [8]. First of all, these curves can be used to determine the breakdown voltages (V_{bd}) of the MRS APDs, which is an important parameter, since it defines the working point of the particular MRS APD, which is about 10-20 % above the breakdown voltage. In addition, the I-V measurement is also useful to identify damaged MRS APDs and to get an estimate for the quality of the particular MRS APD. During the measurements the temperature was stabilized to 20 °C using a Peltier cooling

system. For each voltage step 20 readings of the current were done with a delay of 200 ms.

Figure 3. Different bunches of MRS APD with similar



breakdown voltages.

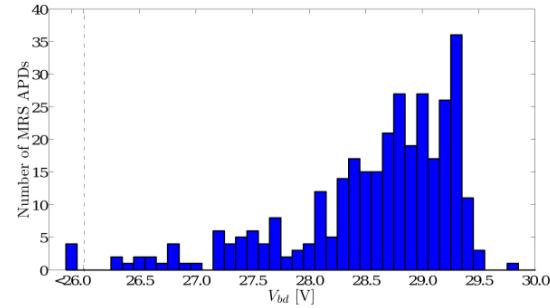


Figure 4: Frequency distribution of the breakdown voltages of 326 tested MRS APDs [8].

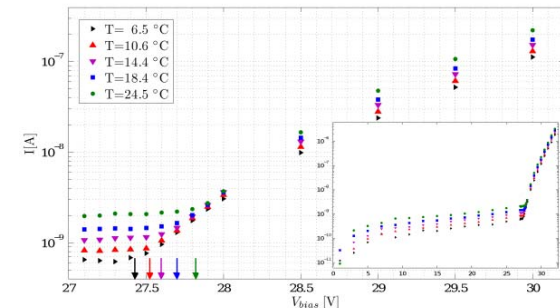


Figure 5: The reverse I-V characteristic of MRS APD #092 at different temperatures (the arrows indicate the breakdown voltages). The small embedded illustration shows the whole I-V curve.

The breakdown voltages and the corresponding leakage currents for each MRS APD were extracted from the I-V curves. Figure 3 shows the reverse I-V curves of different MRS APDs. All characterized MRS APDs are divided into subgroups with similar breakdown voltages. The frequency distribution of the breakdown voltages is shown in figure 4. More than 80 % of the tested MRS

APDs have breakdown voltages in the range of 28.7 ± 0.7 V [8].

For several MRS APDs, the I-V measurements were also carried out for different temperatures. As can be seen in figure 5, the breakdown voltage increases with the temperature.

4 Gain measurements

MRS APDs have an outstanding single photoelectron resolution. As a consequence the peaks corresponding to 0-, 1-, 2-, ... photoelectron (p.e.) signals are clearly separated in the charge distribution as shown in figure 6. By means of these spectra, the gain of the MRS APD can be determined. The intrinsic gain of a MRS APD can be calculated by using the distance between two neighboring peaks in the pulse height spectrum.

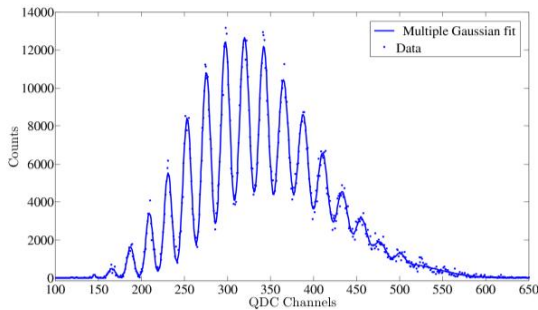


Figure 6: A typical multi p.e. charge spectrum of a MRS APD.

The gain as a function of the overvoltage $\Delta V = V_{\text{bias}} - V_{\text{bd}}$ for six different MRS APDs is diagrammed in figure 7. As expected, the gain depends linearly on the overvoltage.

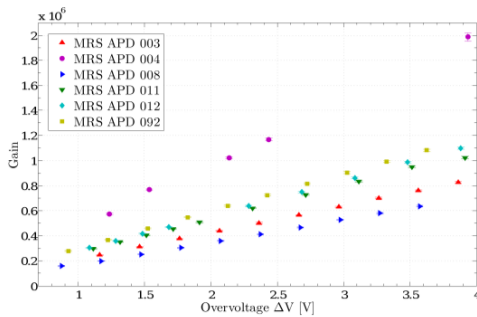


Figure 7: The gain of six different samples of MRS APDs as a function of the overvoltage measured at the temperature of 5.0 °C.

As can be seen in figure 8, the gain increases with lower temperatures at a fixed bias voltage.

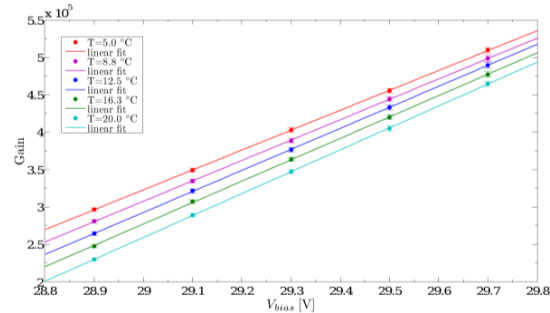


Figure 8: The gain as a function of the bias voltage for different temperatures.

This is due to the fact, that the breakdown voltage decreases with lower temperatures, resulting in a higher overvoltage, and therefore a higher gain. The breakdown voltages for the different temperatures are extracted by linear extrapolation of these curves to zero gain and are plotted as a function of the temperature in figure 9. These data in turn are fitted to linear functions in order to get the temperature gradient dV_{bd}/dT . This temperature gradient is ~ 0.02 V/°C for the measured MRS APDs.

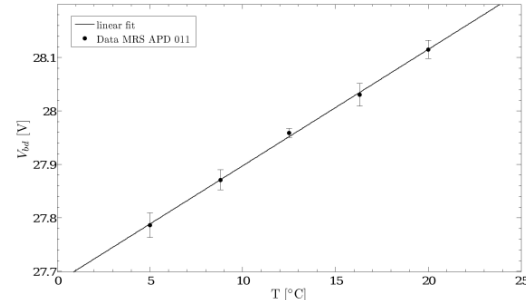


Figure 9: The breakdown voltage as a function of the temperature.

5 Measurements with scintillators

Plastic scintillator tiles will be used to build up two different muon veto systems in the Tuebingen underground laboratory [8].

The scintillator tiles are manufactured by the UNIPLAST company located in Vladimir, Russia. The panels are based on extruded polystyrene with 1.5% PTP (paraphenyl, primary scintillator) and 0.01% POPOP (WLS, secondary scintillator) incorporation. They are etched by a chemical agent, resulting in the formation of a thin white layer (70-100 μ m) over the tile surface [6,7]. This deposit acts as a diffuse reflector layer. The panels are 126 cm long, 20 cm wide and have a thickness of 0.7 cm. The top face contains a U-shaped groove with an embedded wavelength shifting (WLS) fibre from Kuraray¹. The WLS fibre is glued into the groove with a Bicron BC-600

¹ Y11(250)M s-type, $\varnothing = 1$ mm

epoxy optical cement. Both ends of the fibre are coupled with MRS APDs via an optical connector. This configuration should allow a homogeneous light collection over the whole panel area. The panel is wrapped in a diffuse reflecting Tyvek foil in order to enhance the light yield. In addition it is wrapped in pond liner in order to achieve light-tightness. In our measurements the light yield is measured as a function of the position where a minimum ionizing particle (MIP) strikes the scintillator panel. The light yield of the plastic scintillator panel was tested with cosmic ray muons (i.e. MIPs). A PMT-scintillator based trigger setup which can be moved along the scintillator panel is used in order to define an area of impact. The trigger setup consists of two small scintillator tiles with a size of $20 \times 10 \text{ cm}^2$ and each tile is coupled to PMTs² via light guides on both narrow sides. One of these scintillator trigger tiles is placed above, and the other below the scintillator panel. The distance between these two tiles is $\sim 80 \text{ cm}$. An incident cosmic ray muon crossing both trigger tiles then defines a muon event if the coincidence condition is true. Due to the coincidence condition, the electromagnetic background is reduced. In order to determine the light yield, muon spectra were taken using a QDC. The low charge part of the spectrum due to radioactivity background was fitted to Gaussians and the muon peak was fitted to Moyal-functions [9] in order to get the most probable value for the energy loss (in units of QDC channels) for a MIP event. The Moyal-function is an analytical approximation of the Landau-Vavilov distribution [10] which describes the energy loss distribution in thin absorbers and is given by:

$$M = a \cdot \exp(-(\lambda + \exp(-\lambda))/2)$$

where $\lambda = (\mu - \mu_{\text{mp}})/b$, μ_{mp} is the most probable value and b is a constant depending on the absorber [11].

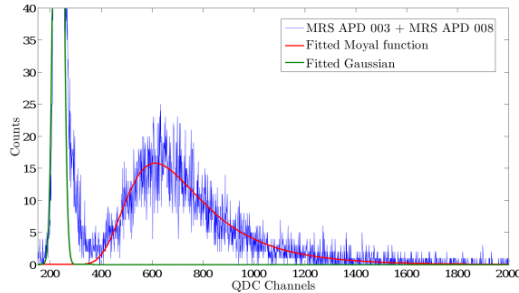


Figure 10: Cosmic ray muon spectrum. The peak due to muon corresponds to a light output of $\sim 25 \text{ p.e.}$

A typical charge spectrum of the scintillator panels due to cosmic muons is shown in figure 10. The peak due to muon corresponds to a light output of $\sim 25 \text{ p.e.}$ It can be seen, that the muon peak is clearly separated from the low energy part due to radioactivity background with a peak-to-valley ratio of ~ 4 . Measurements have shown

that the light yield at the far end of the tile is reduced by about 20 % [8].

6 Conclusion

Extensive studies of MRS APDs parameters demonstrated their good performance, robustness and suitability for use in plastic scintillator panels readout for muon veto detectors of underground cryogenic experiments.

7 Acknowledgements

The work has been supported by project SFB #TR27 by DFG.

8 References

- [1] Z. Sadygov, 1998, Russian Agency for Patents and Trademarks, Patent No. RU 2102820.
- [2] V. Golovin, 1999, Russian Agency for Patents and Trademarks, Patent No. RU 2142175.
- [3] D. McNally, V. Golovin, Nuclear Instruments and Methods A, 2009, 610: 150-153.
- [4] Z. Sadygov et al., Nuclear Instruments and Methods A, 2006, **567**: 70.
- [5] D. Renker, E. Lorenz, Journal of Instrumentation, 2009, **4**, P04004.
- [6] A. Akindinov et al., Nuclear Instruments and Methods A, 2005, **539**: 172.
- [7] Yu. Musienko et al., Instruments and Experimental Techniques, 2008, **51**(1), 101-107.
- [8] R. Falkenstein, Diploma Thesis, University of Tuebingen, 2011.
- [9] J.E. Moyal, Phil. Mag. 1955, **46**: 263.
- [10] L.D. Landau, J.Phys.(USSR) **8**: 201.
- [11] T. Davidek, R. Leitner, Atlas note, 1997, ATL-TILECAL-97-114.